MOLECULAR PHARMACOLOGY, 23:133–140

Correlation of Structure and Activity in Ansamycins

Molecular Structure of Sodium Rifamycin SV

S. K. ARORA

Department of Chemistry, University of Arizona, Tucson, Arizona 85721

Received June 14, 1982; Accepted August 30, 1982

SUMMARY

The crystal and molecular structure of the sodium salt of rifamycin SV (clinically known as rifacin) as the monohydrate ethanol solvate has been determined to study the conformation of the *ansa* chain in unsubstituted rifamycins and also to clarify the metal complexation with rifamycins. The crystals belong to the space group $P2_12_12_1$ with cell dimensions (estimated standard deviations in parentheses) of a = 12.061 (2), b = 13.936 (2), and c = 24.731 (4) Å. The structure was solved by direct methods and refined to an R factor of 0.069. The conformation of the *ansa* chain differs from that of other active rifamycins, e.g., rifampcin and rifamycin B at the joining point of the *ansa* chain to the naphthohydroquinone chromophore. The conformation of the middle part of the *ansa* chain, which is essential for activity against DNA-dependent RNA polymerase, remains the same. The sodium ion is penta-coordinated and has a trigonal bipyramidal geometry. The intermolecular hydrogen bonding involves O(9), O(10), O(5), and O(6) through water and ethanol molecules. A two-step mode of action of rifamycins has been postulated, and the conformations of antibiotics suitable for penetration of the membrane barrier and that for antibiotic-enzyme complex formation have been suggested.

INTRODUCTION

Rifamycins are a group of antibiotics produced by the chemical modification of the fermentation broth of *Streptomyces mediterranei* (1). They are naphthalenic ansamycins having a 17-membered *ansa* chain. They have activity against a large variety of organisms, such as bacteria, eukaryotes, and viruses, and for that reason they are sometimes called "wonder drugs." The antimicrobial activity of rifamycins against Gram-positive and Gram-negative bacteria is due to the inhibition of RNA synthesis catalyzed by DDRP[1] (2, 3). These antibiotics are used in particular for the treatment of tuberculosis. Rifamycins have also shown antitumor activity when injected during the growth of experimental tumors (4).

RIFAB, the original compound isolated, has no activity but is oxidized easily to rifamycin O. Rifamycin S is obtained by the hydrolysis of rifamycin O. RIFASV and rifamycin S are the reduced and oxidized forms, respectively, of the reversible oxidation-reduction system involving two electrons (Fig. 1). RIFASV in its water-soluble, injectable sodium salt was the first rifamycin to find clinical applications in several countries (7).

A great number of chemical modifications to the structure of rifamycins have been made, mostly at position 3 or 4 of the naphthoquinone or naphthohydroquinone chromophore. RIFAMP, a very active rifamycin, is a semisynthetic derivative of rifamycin SV. Any modification in the *ansa* bridge generally reduces the activity. Many studies on the relationship of structural features with the activity of these antibiotics have been carried out (5–8). From these studies, it seems that the antibacterial activity is dependent upon the presence of (a) a naphthalene ring carrying two oxygen atoms [either in quinone form or as free hydroxyl groups at C(1) and C(8)], (b) two unsubstituted hydroxyls on C(21) and C(23) in the *ansa* chain, and (c) a well-defined spatial arrangement of oxygen atoms at C(21) and C(23).

Until now all of the crystal structure studies of rifamycins have involved either 3- or 4-substitutions [e.g., RIFAMP (9), RIFAB *p*-iodoanilide (5), and CMRS (10)] or those with changes in the *ansa* chain (thus inactive) [e.g., tolypomycinone (11) and rifamycin S iminomethyl ether (8)]. This study presents the first structural analysis of a metal complex of an active rifamycin without any substitution.

MATERIALS AND METHODS

RIFASV[2] was obtained from P-L Biochemicals (Milwaukee, Wisc.). Red needle-shaped crystals were ob-

This work was supported by Grant GM25150 from the National Institutes of Health.

[1] The abbreviations used are: DDRP, DNA-dependent RNA polymerase; RIFAB, rifamycin B; RIFASV, rifamycin SV; RIFAMP, rifampcin; CMRS, 3-carbomethoxy rifamycin S.

[2] Rifamycin SV as listed in the supplier's catalogue is actually the sodium salt of RIFASV.

0026-895X/83/010133-08$02.00/0

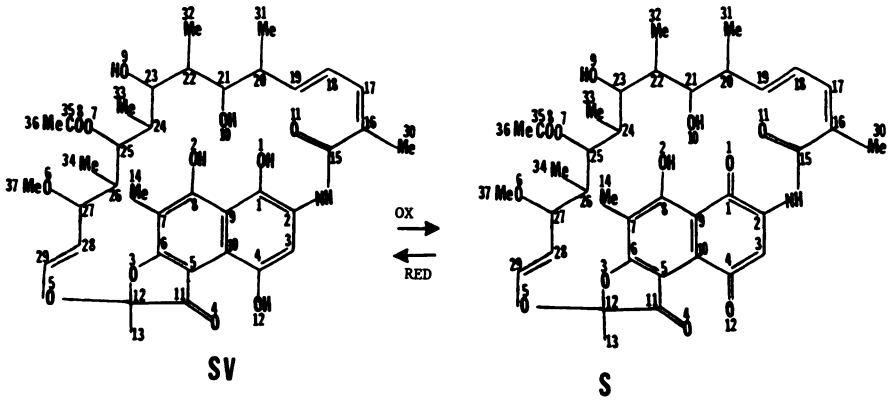

FIG. 1. *Chemical formulae and interconversion of rifamycins SV and S*

tained from aqueous methanol after several unsuccessful attempts. A crystal measuring 0.2 × 0.2 × 0.3 mm was used for the measurement of cell constants and data collection. The crystals belonged to the orthorhombic space group $P2_12_12_1$ with cell dimensions (estimated standard deviations in parentheses) of a = 12.061 (2), b = 13.936 (2), and c = 24.731 (4) Å; Z = 4; D_{meas} = 1.243 (CCl_4/petroleum ether), D_{calc} = 1.238 g cm^{-3}; Fw = 774.77; V = 4156.8 Å^3. The intensities of 2853 unique reflections with $2\theta < 105°$ were measured using CuKα radiation (λ=1.5418 Å) on a Syntex P3/F diffractometer, using a θ-2θ scan technique, a variable scan rate (0.5–29.3 min), a scan range of 2.0°, and a background-to-scan ratio of 0.8; 1869 reflections > 3σ(I) were considered observed. The intensities were corrected for Lorentzian and polarization effects. The unit cell parameters were obtained by least-squares fittings of the settings of four angles of 25 reflections.

The structure was solved by the direct-method program MULTAN 78 (12) after several unsuccessful attempts. Altogether 399 E values > 1.5 were used. The first E map revealed 40 atoms. At first the top peak in the map was rejected as spurious (since the compound was supposed to be just RIFASV), but later it was found to be that of the sodium atom. The structure was refined isotropically to R of 0.192. At this stage a difference Fourier map revealed the presence of a water molecule and ethanol as solvents. Further isotropic and anisotropic

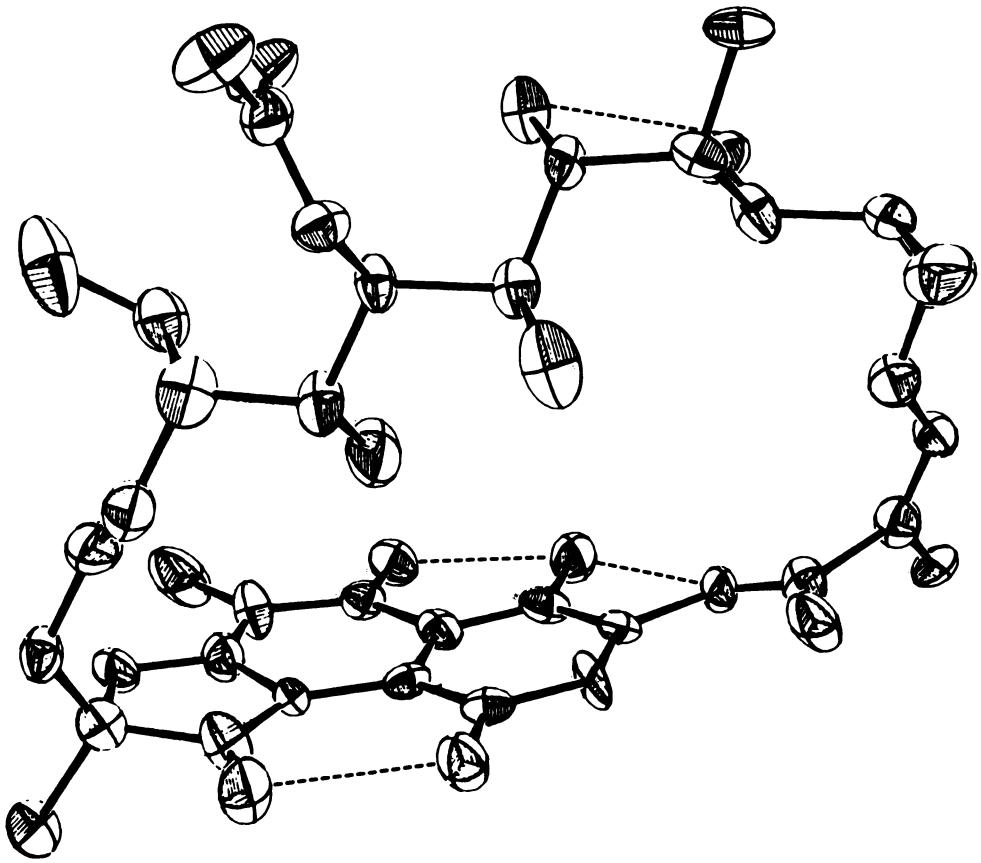

FIG. 2. *Thermal ellipsoid plot of the molecule*
Intramolecular hydrogen bonds are depicted by - - -.

TABLE 1

Atomic coordinates for non-hydrogen atoms

Values are × 10^4, with estimated standard deviations in parentheses.

Atom	X	Y	Z
Na	−6,284 (3)	4,458 (3)	3,535 (2)
O(1)	−11,016 (7)	1,715 (6)	3,149 (3)
O(2)	−11,617 (7)	−18 (6)	3,060 (3)
O(3)	−9,177 (6)	−2,511 (6)	3,511 (3)
O(4)	−6,621 (7)	−1,329 (6)	3,675 (4)
O(5)	−7,864 (7)	−2,905 (5)	4,171 (3)
O(6)	−9,464 (7)	−1,506 (5)	5,454 (3)
O(7)	−8,053 (7)	7 (5)	6,260 (3)
O(8)	−9,678 (7)	−327 (5)	6,648 (3)
O(9)	−10,107 (7)	1,753 (6)	6,164 (3)
O(10)	−10,488 (7)	3,399 (6)	5,664 (3)
O(11)	−7,943 (7)	3,702 (6)	3,695 (4)
O(12)	−6,759 (6)	504 (6)	3,604 (4)
O(13)	−6,643 (8)	4,414 (7)	2,592 (3)
O(1)	−6,438 (8)	5,373 (6)	4,348 (3)
N	−9,476 (8)	2,991 (7)	3,386 (4)
C(1)	−9,967 (9)	1,381 (9)	3,255 (4)
C(2)	−9,139 (9)	2,025 (8)	3,360 (5)
C(3)	−8,068 (9)	1,703 (8)	3,465 (5)
C(4)	−7,832 (9)	759 (9)	3,487 (4)
C(5)	−8,503 (9)	−958 (8)	3,450 (4)
C(6)	−9,425 (9)	−1,577 (9)	3,409 (5)
C(7)	−10,485 (9)	−1,326 (9)	3,291 (5)
C(8)	−10,651 (9)	−0,313 (9)	3,195 (4)
C(9)	−9,751 (9)	387 (8)	3,274 (4)
C(10)	−8,641 (8)	66 (8)	3,391 (4)
C(11)	−7,608 (9)	−1,508 (8)	3,580 (5)
C(12)	−7,993 (9)	−2,575 (9)	3,640 (5)
C(13)	−7,471 (9)	−3,270 (9)	3,265 (5)
C(14)	−11,400 (9)	−2,034 (9)	3,235 (6)
C(15)	−8,914 (9)	3,731 (8)	3,569 (5)
C(16)	−9,604 (8)	4,679 (8)	3,622 (5)
C(17)	−9,711 (8)	5,065 (8)	4,109 (4)
C(18)	−9,290 (9)	4,664 (8)	4,614 (4)
C(19)	−9,519 (9)	5,037 (9)	5,101 (5)
C(20)	−9,072 (9)	4,648 (9)	5,621 (5)
C(21)	−9,290 (9)	3,554 (8)	5,678 (4)
C(22)	−8,776 (9)	3,085 (9)	6,184 (5)
C(23)	−8,931 (8)	2,000 (8)	6,188 (4)
C(24)	−8,369 (9)	1,469 (8)	5,716 (5)
C(25)	−8,594 (9)	343 (8)	5,769 (5)
C(26)	−8,149 (9)	−244 (8)	5,297 (5)
C(27)	−8,285 (9)	−1,303 (8)	5,411 (4)
C(28)	−7,821 (9)	−1,922 (8)	4,946 (5)
C(29)	−8,373 (9)	−2,341 (9)	4,568 (5)
C(30)	−10,084 (9)	5,070 (9)	3,121 (6)
C(31)	−7,805 (9)	4,869 (9)	5,669 (6)
C(32)	−9,177 (10)	3,519 (10)	6,696 (5)
C(33)	−7,083 (9)	1,656 (9)	5,691 (5)
C(34)	−8,761 (9)	92 (9)	4,775 (5)
C(35)	−8,699 (9)	−296 (9)	6,675 (4)
C(36)	−8,063 (9)	−574 (9)	7,155 (5)
C(37)	−9,649 (9)	−2,347 (9)	5,772 (5)
C(38)	−5,809 (15)	4,004 (15)	2,227 (8)
C(39)	−5,416 (24)	3,102 (16)	2,371 (9)

refinement of atomic and thermal parameters of non-hydrogen atoms reduced R to 0.085. Thirty-six hydrogen atoms were located from a difference map, and the rest of the hydrogen positions were calculated. After including hydrogen atoms, and refining non-hydrogen atoms anisotropically and hydrogen atoms isotropically, the final R value dropped to 0.069. The refinement was based on Fo, the quantity minimized being $\sum(Fo-Fc)^2$. The scattering factors used were those of Hanson *et al.* (13). The final atomic coordinates for nonhydrogen atoms are given in Table 1.

RESULTS

Bond lengths and bond angles are given in Table 2 and 3. There was good agreement between the values found in RIFASV and those found in RIFAMP (except those involving the amino N atom). This may have been due to a conformational difference in that area. The bond distances (estimated standard deviations in parentheses) in the ethanol molecule were C(38)—C(39) = 1.39 (1) and C(39)—O(13) = 1.47 (1) Å. The bond distances involving hydrogen atoms had values between 0.80 and 1.20 Å. The bond angles for hydrogen atoms varied between 95° and 120°.

The stereochemistry of a RIFASV molecule is shown in Fig. 2. The molecule consists of a near-planar part formed by the naphthohydroquinone nucleus with a 5-membered ring condenses to it, and a 17-membered *ansa* chain that is connected to C(2) and C(12). The mean deviation for the best plane through C(1)—C(10) is 0.02 Å. The dihedral angle between the naphthohydroquinone

TABLE 2

Bond lengths

The standard deviations are of the order of 0.01 Å.

Bond	Length	Bond	Length
	Å		Å
C(1)—C(2)	1.37	C(20)—C(31)	1.56
C(1)—C(9)	1.41	C(21)—C(22)	1.54
C(1)—O(1)	1.37	C(21)—O(10)	1.46
C(2)—C(3)	1.39	C(22)—C(23)	1.52
C(2)—N	1.41	C(22)—C(32)	1.48
C(3)—C(4)	1.35	C(23)—C(24)	1.54
C(4)—C(10)	1.39	C(23)—O(9)	1.46
C(4)—O(12)	1.37	C(24)—C(25)	1.59
C(5)—C(6)	1.41	C(24)—C(33)	1.60
C(5)—C(10)	1.44	C(25)—C(26)	1.52
C(5)—C(11)	1.36	C(25)—O(7)	1.46
C(6)—C(7)	1.36	C(26)—C(27)	1.51
C(6)—O(3)	1.36	C(26)—C(34)	1.56
C(7)—C(8)	1.44	C(27)—C(28)	1.54
C(7)—C(14)	1.49	C(27)—O(6)	1.45
C(8)—C(9)	1.47	C(28)—C(29)	1.29
C(8)—O(2)	1.28	C(29)—O(5)	1.40
C(9)—C(10)	1.44	C(35)—C(36)	1.46
C(11)—C(12)	1.56	C(35)—O(7)	1.36
C(11)—O(4)	1.24	C(35)—O(8)	1.18
C(12)—C(13)	1.48	C(37)—O(6)	1.43
C(12)—O(3)	1.47	C(38)—C(39)	1.39
C(12)—O(5)	1.40	C(38)—O(13)	1.47
C(15)—C(16)	1.57		
C(15)—N	1.31		
C(15)—O(11)	1.21		
C(16)—C(17)	1.32		
C(16)—C(30)	1.47		
C(17)—C(18)	1.46		
C(18)—C(19)	1.34		
C(19)—C(20)	1.50		
C(20)—C(21)	1.55		

TABLE 3

Bond angles

The standard deviations are of the order of 0.7°.

Atoms	Angle	Atoms	Angle
C(2)—C(1)—C(9)	120.2°	C(17)—C(18)—C(19)	123.4°
C(2)—C(1)—O(1)	119.1	C(18)—C(19)—C(20)	124.0
C(9)—C(1)—O(1)	120.6	C(19)—C(20)—C(21)	111.9
C(1)—C(2)—C(3)	120.1	C(19)—C(20)—C(31)	110.2
C(1)—C(2)—N	115.1	C(21)—C(20)—C(31)	110.6
C(3)—C(2)—N	124.6	C(20)—C(21)—C(22)	115.0
C(2)—C(3)—C(4)	121.2	C(20)—C(21)—O(10)	108.1
C(3)—C(4)—C(10)	121.7	C(22)—C(21)—O(10)	110.8
C(3)—C(4)—O(12)	117.4	C(21)—C(22)—C(23)	112.1
C(10)—C(4)—O(12)	121.0	C(21)—C(22)—C(32)	112.9
C(6)—C(5)—C(10)	120.6	C(23)—C(22)—C(32)	111.0
C(6)—C(5)—C(11)	107.3	C(22)—C(23)—C(24)	114.8
C(10)—C(5)—C(11)	131.9	C(22)—C(23)—O(9)	110.7
C(5)—C(6)—C(7)	126.8	C(24)—C(23)—O(9)	106.5
C(5)—C(6)—O(3)	113.6	C(23)—C(24)—C(25)	109.6
C(7)—C(6)—O(3)	119.6	C(23)—C(24)—C(33)	112.5
C(6)—C(7)—C(8)	114.7	C(25)—C(24)—C(33)	109.5
C(6)—C(7)—C(14)	123.2	C(24)—C(25)—C(26)	113.9
C(8)—C(7)—C(14)	122.0	C(24)—C(25)—O(7)	108.0
C(7)—C(8)—C(9)	121.5	C(26)—C(25)—O(7)	108.0
C(7)—C(8)—O(2)	118.9	C(25)—C(26)—C(27)	110.1
C(9)—C(8)—O(2)	119.5	C(25)—C(26)—C(34)	107.8
C(1)—C(9)—C(8)	120.7	C(27)—C(26)—C(34)	113.3
C(1)—C(9)—C(10)	118.8	C(26)—C(27)—C(28)	111.6
C(8)—C(9)—C(10)	120.4	C(26)—C(27)—O(6)	108.1
C(4)—C(10)—C(5)	126.4	C(28)—C(27)—O(6)	107.6
C(4)—C(10)—C(9)	117.9	C(27)—C(28)—C(29)	127.3
C(5)—C(10)—C(9)	115.6	C(28)—C(29)—O(5)	122.6
C(5)—C(11)—C(12)	108.8	C(36)—C(35)—O(7)	113.3
C(5)—C(11)—O(4)	133.8	C(36)—C(35)—O(8)	124.0
C(12)—C(11)—O(4)	117.3	O(7)—C(35)—O(8)	122.7
C(11)—C(12)—C(13)	115.8	C(2)—N—C(15)	128.1
C(11)—C(12)—O(3)	102.2	C(6)—O(3)—C(12)	108.2
C(11)—C(12)—O(5)	111.6	C(12)—O(5)—C(29)	115.2
C(13)—C(12)—O(3)	108.5	C(27)—O(6)—C(37)	110.6
C(13)—C(12)—O(5)	109.0	C(25)—O(7)—C(35)	118.3
O(3)—C(12)—O(5)	109.3	C(39)—C(38)—O(13)	115.3
C(16)—C(15)—N	114.6		
C(16)—C(15)—O(11)	121.3		
N—C(15)—O(11)	124.1		
C(15)—C(16)—C(17)	118.1		
C(15)—C(16)—C(30)	116.7		
C(17)—C(16)—C(30)	125.2		
C(16)—C(17)—C(18)	126.1		

ring and the 5-membered ring attached to it is 8.0. In the *ansa* chain the C(16)—C(17) and C(18)—C(19) double bond are *cis* and *trans*, respectively, and their conformations are transoid with respect to the C(17)—C(18) single bond. The C(28)—C(29) double bond has a *trans* configuration.

TABLE 4

Distances between O(1), O(2), O(9), and O(10) in RIFASV, RIFAMP, RIFAB, and CMRS

Atoms	RIFASV	RIFAMP	RIFAB	CMRS
	Å	Å	Å	Å
O(1)—O(2)	2.5	2.5	2.6	2.5
O(1)—O(9)	7.5	6.2	6.7	7.0
O(1)—O(10)	6.7	5.4	5.7	5.8
O(2)—O(9)	8.3	6.8	7.8	7.4
O(2)—O(10)	8.1	6.9	7.5	7.0
O(9)—O(10)	2.6	2.7	2.7	2.7

TABLE 5

Torsion angles along the skeleton of the ansa chain in RIFASV, CMRS, RIFAB, and RIFAMP

	RIFASV	CMRS	RIFAB	RIFAMP
C(1)—C(2)—N—C(15)	167°	−141°	−32°	−55°
C(2)—N—C(15)—C(16)	−171	177	180	179
N—C(15)—C(16)—C(17)	119	63	−43	−31
C(15)—C(16)—C(17)—C(18)	−3	2	5	4
C(16)—C(17)—C(18)—C(19)	−173	169	168	155
C(17)—C(18)—C(19)—C(20)	−179	−179	−175	−165
C(18)—C(19)—C(20)—C(21)	−52	−30	−11	−19
C(19)—C(20)—C(21)—C(22)	176	180	170	169
C(20)—C(21)—C(22)—C(23)	−175	−178	−179	−176
C(21)—C(22)—C(23)—C(24)	62	57	53	62
C(22)—C(23)—C(24)—C(25)	180	−174	174	165
C(23)—C(24)—C(25)—C(26)	176	169	155	159
C(24)—C(25)—C(26)—C(27)	174	180	174	153
C(25)—C(26)—C(27)—C(28)	−179	180	−170	−171
C(26)—C(27)—C(28)—C(29)	−101	−110	117	118
C(27)—C(28)—C(29)—O(5)	−179	−176	−168	−175
C(28)—C(29)—O(5)—C(12)	−118	−127	49	65
C(29)—O(5)—C(12)—O(3)	−58	−52	−79	−78

The over-all conformation of the RIFASV molecule is compared with that of other highly active rifamycins, e.g., RIFAB, RIFAMP, and CMRS (which has high activity in isolated DDRP) in Figs. 3–5. The least-squares plane containing the 17 atoms of the *ansa* chain and that containing 10 atoms of the chromophore make an angle of 75.1° in RIFASV. The similar angles in RIFAB and RIFAMP have values of 109.2° and 98.3°.

The spatial arrangement of four oxygen atoms [O(1), O(2), O(9), and O(10)], which is supposed to be an important factor in the binding of the antibiotics to DDRP, displays a common pattern in all active rifamycins, e.i., RIFAB, RIFAMP, and CMRS (which is active on isolated DDRP) (Figs. 3–5). The spatial distances between these four oxygen atoms in RIFASV and their comparison with similar distances in other rifamycins are given in Table 4. The distances in RIFASV are larger than in any other active rifamycin. As can be seen from Fig. 2, the oxygen atoms O(9) and O(10) lie on the same side of O(1) and O(2) with respect to the best plane containing the *ansa* bridge with bonds C(23)—O(9) and C(21)—O(10), which are nearly perpendicular to the plane. Figure 6 shows the spatial requirement for the activity against DDRP.

The conformation of the *ansa* chain in RIFASV differs most from RIFAB and RIFAMP near the junction of the *ansa* chain and the chromophore at C(2). The torsion angles C(1)—C(2)—N—C(15) and N—C(15)—C(16)—C(17) have values of 167° and 119°, whereas the values observed in RIFAB and RIFAMP for these angles are −32°, −43°, −55°, and −31°, respectively. These differences cause the reversal of amide and carbonyl groups. As also observed in CMRS, the remaining difference in the conformation of the *ansa* chain arises at the other end, where the *ansa* chain joins the chromophore at C(12). The torsion angles C(26)—C(27)—C(28)—C(29) and C(28)—C(29)—O(5)—C(12) have values of −101°

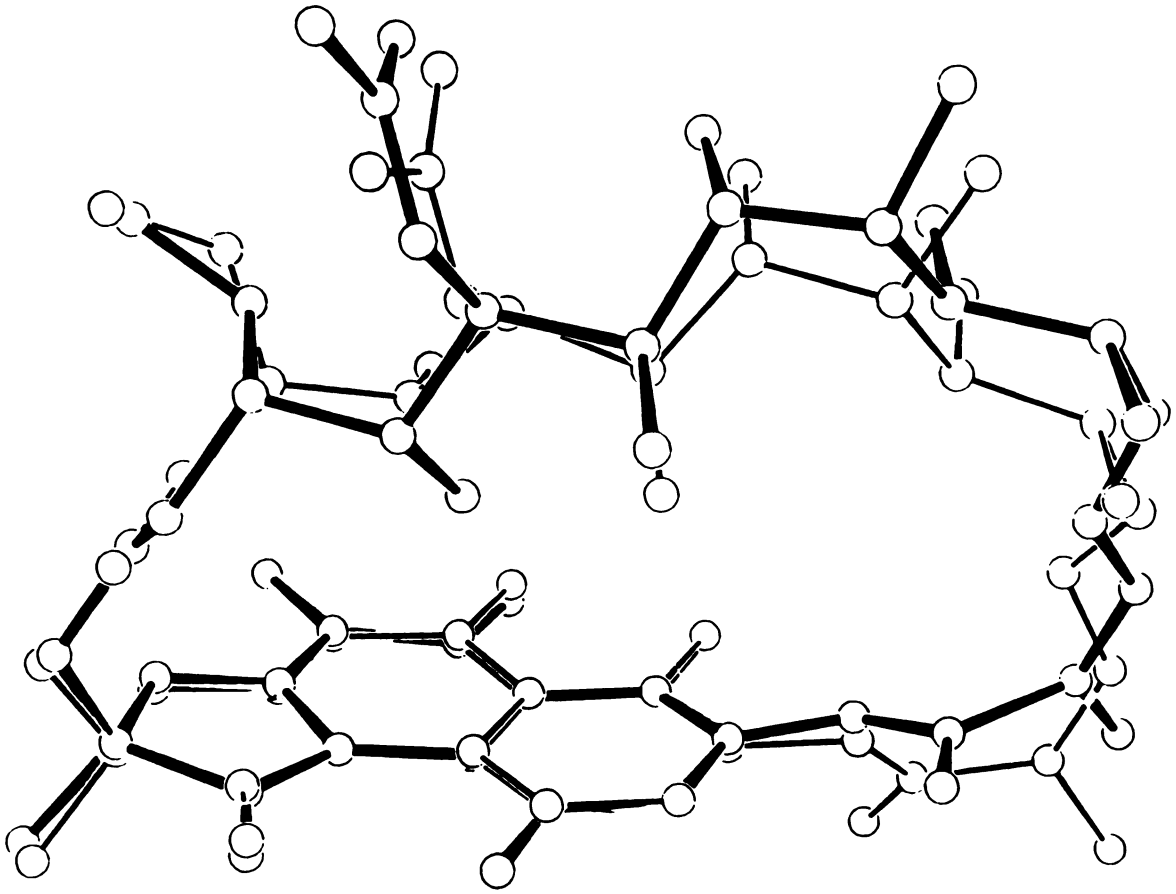

FIG. 3. *Comparison of conformations of RIFASV and RIFAMP (thin bonds)*

and −118°. These are very close to values for CMRS (−110° and 112°) but quite different from those of RIFAB (117° and 49°) and RIFAMP (118° and 65°). The other torsion angles in the *ansa* chain are very similar in all active rifamycins (Table 5).

Figure 7 shows the packing of the molecules looking down the *c* axis. The molecules form channels approximately parallel to the *b* axis and the sodium atom; water and ethanol molecules lie in these channels and form hydrogen bonds. Both O(9) and O(10), which are important for the activity, are involved in hydrogen bonding. Table 6 gives both the intra- and intermolecular hydrogen bond distances. The coordination of the metal ion is depicted in Fig. 8. Usually sodium ion exhibits distorted octahedral coordination (14), whereas in the present compound it is penta-coordinated and the values of bond lengths and angles are close to those expected in penta-coordinated sodium ions (15–17). The over-all geometry is trigonal bipyramidal.

TABLE 6

Hydrogen bonds

Donor atom	Acceptor atom	Distance	Symmetry of acceptor
		Å	
O(1)	O(2)	2.53	x, y, z
O(2)	O(13)	2.76	$2 - x, -\frac{1}{2} + y, \frac{1}{2} - z$
N	O(1)	2.64	x, y, z
O(9)	O(10)	2.65	x, y, z
O(10)	O(12)	2.82	$\frac{1}{2} + x, \frac{1}{2} - y, 1 - z$
O(12)	O(4)	2.57	x, y, z
OW	O(5)	2.90	$x, 1 + y, z$
OW	O(6)	2.99	$-\frac{1}{2} + x, \frac{1}{2} - y, 1 - z$

DISCUSSION

It is known that RIFASV has high activity against Gram-positive bacteria and very little against Gram-negative bacteria. The reason for the latter is that the antibiotic is unable to enter the cell. This has also been found in some other rifamycins. In fact, CMRS is very active against isolated DDRP but its antibacterial activity is very low. This leads to the conclusion that antibiotic action is a two-step process, the first being overcoming the membrane barrier to cell entry and the second being the antibiotic-enzyme (DDRP) complex formation.

From the structural studies of active rifamycins conducted thus far, two types of conformations (Fig. 9) at the junction of the chromophore with the *ansa* chain at C(2) are observed. RIFAMP and RIFAB have conformations close to **I**, whereas RIFASV and CMRS are closer to Conformation **II**. Conformation **I** in RIFAMP is probably due to the presence of the electron-accepting group (3-formylhydrazone), which is involved in hydrogen bonding with the —NH group of the *ansa* chain. I suggest that Conformation **I** is the preferred conformation for crossing the membrane to enter the cell. One reason is that in this conformation the antibiotic would

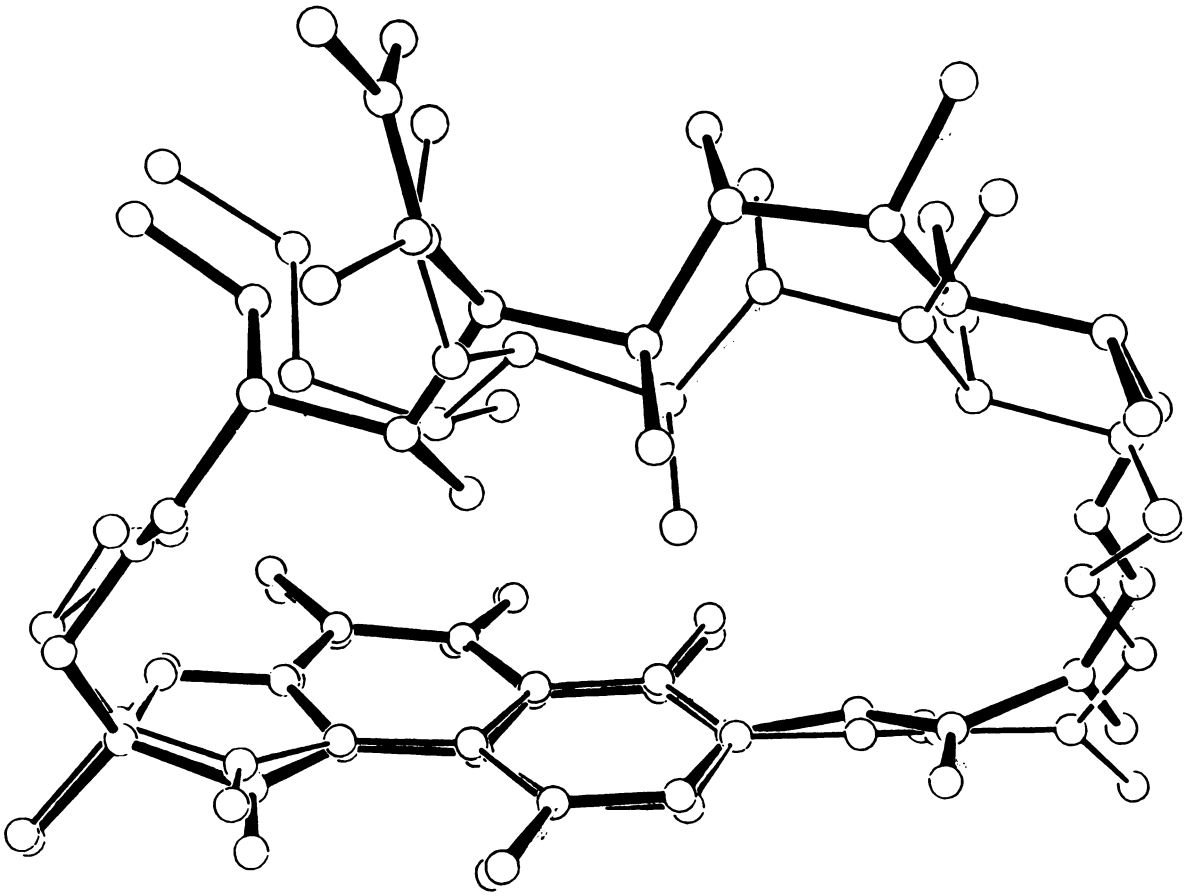

FIG. 4. *Comparison of the conformations of RIFASV and RIFAB (thin bonds)*

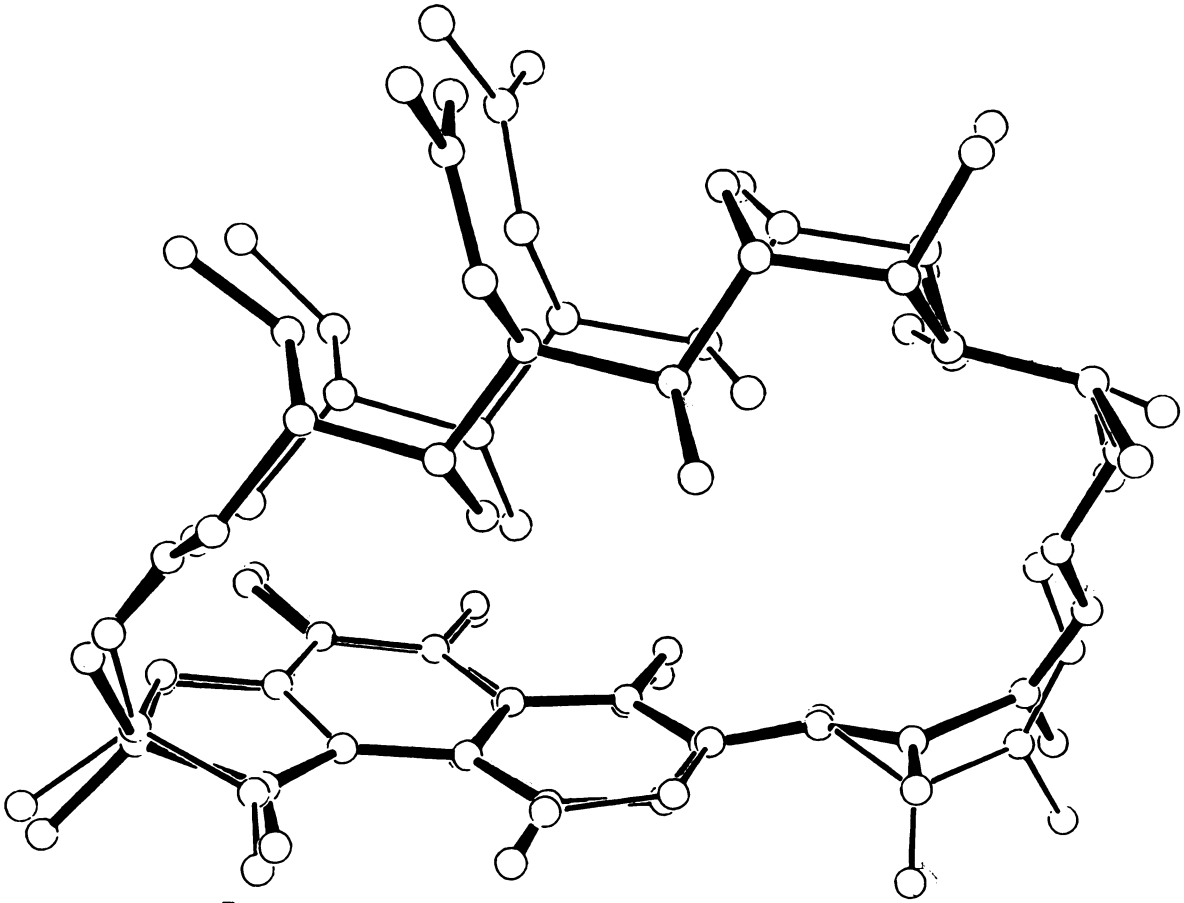

FIG. 5. *Comparison of the conformations of RIFASV and CMRS (thin bonds)*

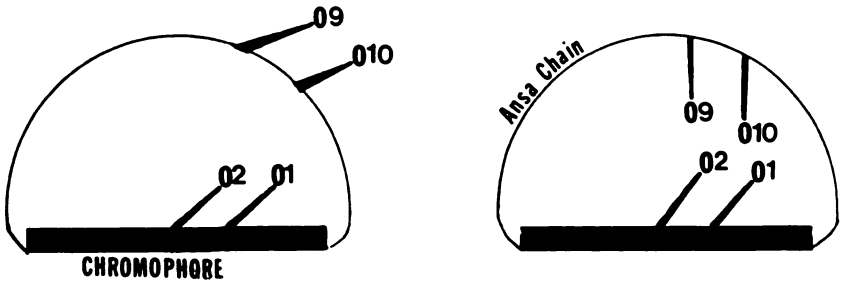

FIG. 6. *Spatial arrangement of O(1), O(2), O(9), and O(10) in active (left) and inactive (right) rifamycins*

be in favorable conformation to form stable alkali metal ion complexes involving O(1), O(2), O(9), O(10), O(11), and perhaps O(8) (Fig. 10). This complex will be very compact and will keep the *ansa* chain conformation stable. This could facilitate diffusion across the membrane. After crossing the membrane, the metal ion could be released and the antibiotic could adopt either Conformation I or Conformation II. It is also possible that Conformation I may be preferred in forming complexes with membrane protein which will make the antibiotic lipid-soluble and thus pass the membrane. In the present study the sodium ion is complexed to two different molecules of antibiotic, making it very bulky and thus slowing down the rate of diffusion across the membrane.

Once the antibiotics have crossed the membrane, the conformation of the drug could be either I or II, since the essential element for the formation of antibiotic-enzyme complex is the spatial geometry of O(1), O(2), O(9), O(10). As a matter of fact, in the complex formation Conformation II may be slightly preferred. The antibiotic-enzyme complex formation most probably involves π-π interactions between the chromophore (naphthoquinone or naphthohydroquinone) and the aromatic amino acids of the β-unit of the enzyme (DDRP) and hydrogen bonding. The greater the distance between O(1)—O(10) and O(2)—O(9), the easier it is for aromatic amino acids and the chromophore to stack. The distances in RIFASV and CMRS (Conformation II) are larger than those observed in RIFAB and RIFAMP. The hydrogen bond formation between O(9) and O(10) of the antibiotic and

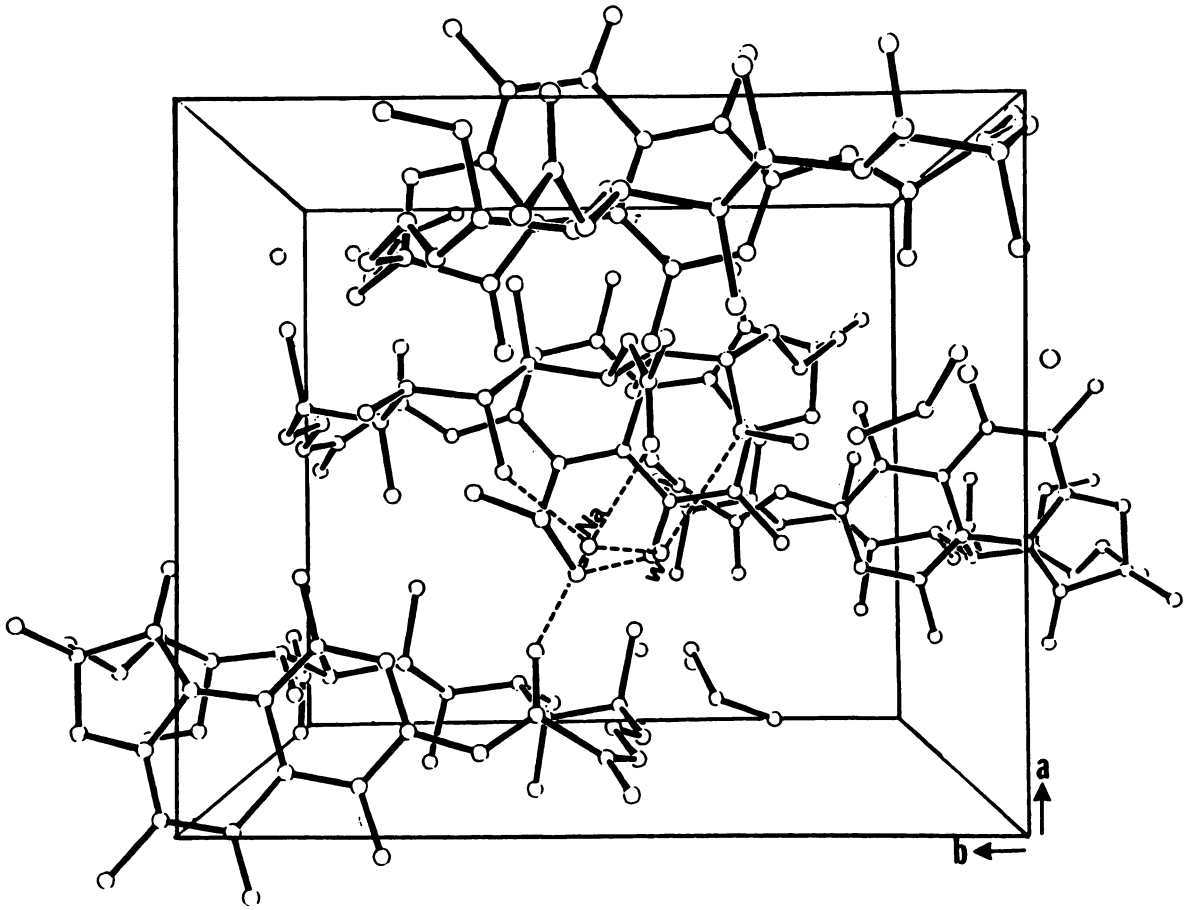

FIG. 7. *Packing of the molecules in the unit cell with c axis vertical*

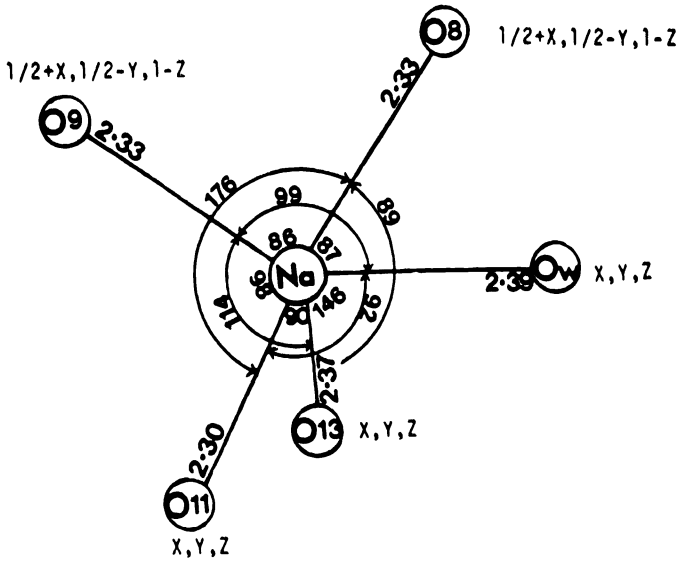

FIG. 8. *Coordination of sodium ions*

enzyme will not be affected. This is a possible mechanism to explain the different conformations observed.

Tables of coordinates of hydrogen atoms, bond lengths and angles involving hydrogen atoms, and structural factors are available from the author upon request.

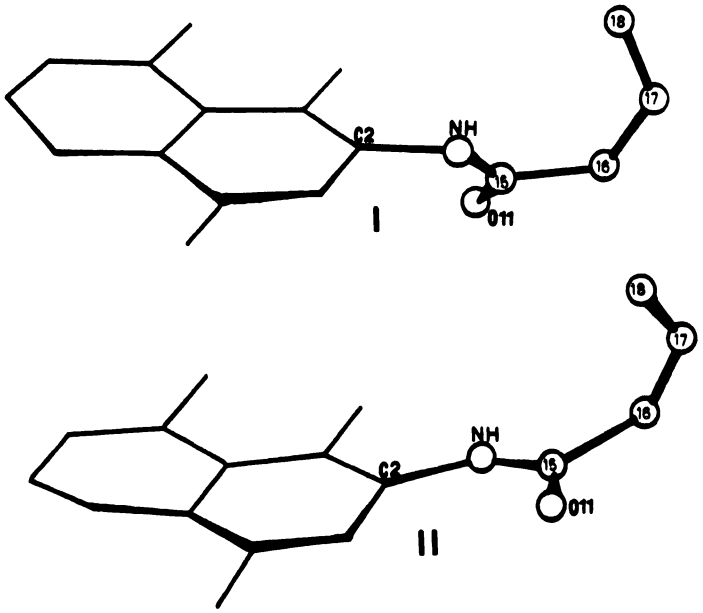

FIG. 9. *Two conformations observed in active rifamycins*

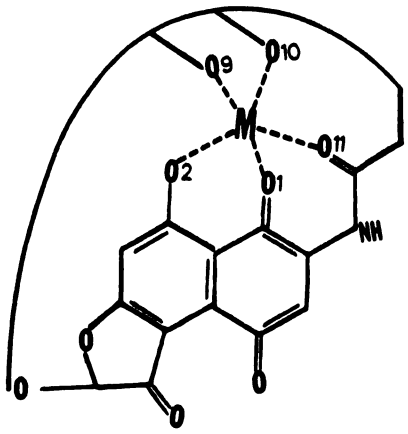

FIG. 10. *Possible coordination of metal ion in complex formation with rifamycins having Conformation I*

REFERENCES

1. Sensi, P., S. Furesz, and G. Maffii. Chemical modifications and biological properties of rifamycins. *Antimicrob. Agents Chemother.* 699–705 (1966).
2. Hartmann, G., K. O. Honikel, F. Knusel, J. Nuesch. The specific inhibition of the DNA-directed RNA synthesis by rifampcin. *Biochim. Biophys. Acta* **145**:843–844 (1967).
3. Umezawa, H., S. Mizuno, H. Yamazaki, K. Nitta. Inhibition of DNA-dependent RNA synthesis by rifamycins. *J. Antibiot. (Tokyo)* **21**:234–236 (1968).
4. Joss, U. R., A. M. Hughes, and H. Calvin. Effect of dimethylbenzyl desmethyl rifampcin on chemically induced mammary tumors in rats. *Nature [New Biol.]* **242**:88–90 (1973).
5. Brufani, M., S. Cerrini, W. Fideli, and A. Vaciago. Rifamycins: an insight into biological activity based on structural investigations. *J. Mol. Biol.* **87**:409–435 (1974).
6. Brufani, M. The ansamycins. *Topics Antibiot. Chem.* **1**:91–212 (1977).
7. Lancini, G., and W. Zanichelli. Structure-activity relationships in rifamycins, in *Structure-Activity Relationships among Semisynthetic Antibiotics.* (D. Perlmann, ed.). Academic Press, New York, 531–600 (1977).
8. Arora, S. K. Structural investigations of mode of action of drugs. III. Structure of rifamycin S iminomethyl ether. *Acta Crystallogr. Sect. B* **37**:152–157 (1981).
9. Gadret, M., M. Gourselle, J. M. Liger, and J. C. Colleter. Structure cristalline de la rifampcine. *Acta Crystallogr. Sect. B* **31**:1454–1462 (1975).
10. Brufani, M., L. Cellai, S. Cerrini, W. Fideli, A. Segree, A. Vaciago. Structure-activity relationships in ansamycins: molecular structure and activity of 3-carbomethoxy rifamycin S. *Mol. Pharmacol.* **21**:394–399 (1982).
11. Brufani, M., L. Cellai, S. Cerrini, W. Fideli, and A. Vaciago. Structure-activity relationships in the ansamycins: the crystal structure of tolypomycinone. *Mol. Pharmacol.* **14**:693–703 (1978).
12. Germain, G., P. Main, and M. M. Woofson. The application of phase relationships to complex structures. *Acta Crystallogr. Sect.* A **27**:368–376 (1971).
13. Hanson, H. P., F. Herman, J. D. Lea, and S. Skillman. HFS atomic scattering factors. *Acta Crystallogr.* **17**:1040–1044 (1964).
14. Shannon, R. D., and C. T. Prewitt. Effective ionic radii in oxides and fluorides. *Acta Crystallogr. Sect. B* **25**:925–946 (1969).
15. Coulter, C. L. Structural chemistry of cyclic nucleotides. *J. Am. Chem. Soc.* **95**:570–575 (1973).
16. James, M. N. G., and G. J. B. Williams. The crystal and molecular structure of disodium maleate monohydrate. *Acta Crystallogr. Sect. B* 1257–1262 (1974).
17. Young, D. W., and H. R. Wilson. The crystal structure of disodium deoxyguanosine-5′-phosphate tetrahydrate. *Acta Crystallogr. Sect. B* **30**:2012–2018 (1974).

Send reprint requests to: Dr. S. K. Arora, Department of Chemistry, University of Arizona, Tucson, Ariz. 85721.